

University of Texas Rio Grande Valley

ScholarWorks @ UTRGV

Manufacturing & Industrial Engineering Faculty
Publications and Presentations

College of Engineering and Computer Science

9-2022

Automated Posture Positioning for High Precision 3D Scanning of a Freeform Design using Bayesian Optimization

Zhaohui Geng

The University of Texas Rio Grande Valley

Bopaya Bidanda

Follow this and additional works at: https://scholarworks.utrgv.edu/mie_fac



Part of the [Industrial Engineering Commons](#), and the [Manufacturing Commons](#)

Recommended Citation

Geng, Zhaohui, and Bopaya Bidanda. "Automated Posture Positioning for High Precision 3D Scanning of a Freeform Design using Bayesian Optimization." *Manufacturing Letters* 33 (2022): 802-807. <https://doi.org/10.1016/j.mfglet.2022.07.099>

This Article is brought to you for free and open access by the College of Engineering and Computer Science at ScholarWorks @ UTRGV. It has been accepted for inclusion in Manufacturing & Industrial Engineering Faculty Publications and Presentations by an authorized administrator of ScholarWorks @ UTRGV. For more information, please contact justin.white@utrgv.edu, william.flores01@utrgv.edu.



50th SME North American Manufacturing Research Conference (NAMRC 50, 2022)

Automated Posture Positioning for High Precision 3D Scanning of a Freeform Design using Bayesian Optimization

Zhaohui Geng^{a*}, Bopaya Bidanda^b^a*Department of Manufacturing and Industrial Engineering, The University of Texas Rio Grande Valley, Edinburg, TX 78539, United States*^b*Department of Industrial Engineering, University of Pittsburgh, Pittsburgh, PA 15261, United States** Corresponding author. E-mail address: zhaohui.geng@utrgv.edu.

Abstract

Three-dimensional scanning is widely used for the dimension measurements of physical objects with freeform designs. The output point cloud is flexible enough to provide a detailed geometric description for these objects. However, geometric accuracy and precision are still debatable for this scanning process. Uncertainties are ubiquitous in geometric measurement due to many physical factors. One potential factor is the object's posture in the scanning region. The posture of target positioning on the scanning platform could influence the normal of the scanning points, which could further affect the measurement variances. This paper first investigates the geometric and spatial factors that could potentially influence scanning variance. This functional relationship is modeled as a Bayesian extreme learning model, which is later utilized to find the object's optimal posture for variance reduction. A Bayesian optimization approach is proposed to solve this minimization problem. Case studies are presented to validate the proposed methodology.

© 2022 Society of Manufacturing Engineers (SME). Published by Elsevier Ltd. All rights reserved.

This is an open access article under the CC BY-NC-ND license (<http://creativecommons.org/licenses/by-nc-nd/4.0/>)

Peer-review under responsibility of the Scientific Committee of the NAMRI/SME.

Keywords: 3D scanning; Point cloud; Geometric metrology; Additive manufacturing; Bayesian optimization.

1. Introduction

Three-dimensional (3D) scanning has attracted extensive research interest in the past decades. It is a technique that surveys geometric information of a physical object and translates it into the digital sphere [1]. Multiple scanning technologies exist and belong to two categories: contact methods and non-contact methods [2]. Contact methods, such as coordinate measuring machines (CMM), provide high accuracy and precision measurements but usually consume a significant amount of time in the geometric information collection [3]. It is therefore usually used to survey the critical dimensions for primitive features or used for applications that require high-precision measurements [4]. Non-contact methods, on the other hand, could collect much more points in a short period of time [5]. Laser scanners, e.g., triangulators or structured light scanners, are widely used in manufacturing

because of their relatively high measurement precision and fast scanning speed [6].

3D scanning is very useful in advanced manufacturing systems, especially those involving mass customization [7, 8] or sustainability [9]. The reverse engineering (RE) [10] and geometric quality inspections [11] are two major applied fields. RE further processes the surveyed geometric information and uses it to build a computer-aided design (CAD) model, which is the *de facto* language in industrial design. This CAD model can be utilized for multiple engineering applications, such as remanufacturing [12], redesign [13], reengineering [14], and simulation [15, 16]. The first and foremost step of an RE process is 3D scanning, where precision will determine the geometric quality for each subsequent step.

Geometric quality inspection using 3D scanning has recently become critical because of the advancement of the additive manufacturing (AM) [17]. AM is a set of manufacturing

processes that share a similar fabrication characteristic—adding material layer by layer [18]. One of the major constraints that hinder the wide adoption of AM is the relatively low geometric accuracy of its produced parts [19]. Therefore, the appropriate metrology tools need to be selected to inspect the AM-produced parts and provide insights into how the process parameters affect the geometric accuracy. The point cloud measured by 3D scanning could provide a detailed description of the AM-printed freeform objects.

Nomenclature

3D	Three-dimensional
RE	Reverse engineering
AM	Additive manufacturing
CAD	Computer-aided design
CCD	Charge-coupled device
BELM	Bayesian extreme learning machine
$f(\cdot)$	The unknown functional relationship between local geometric descriptors and point variance
$\hat{f}(\cdot)$	The estimated functional relationship via Bayesian extreme learning machine
θ_i	The incident angle of the laser stripe
σ_i^2	The variance of the scanned point i
t_i	The logarithm of σ_i^2
v_i	The rate of the local curvature change of point i
R	Rigid rotation matrix
α	Yaw (z -axis) rotation angle
β	Pitch (y -axis) rotation angle
γ	Roll (x -axis) rotation angle
θ^R	The incident angle of the laser stripe after rotation R
\mathbf{n}_i	The normal direction of the point i , $\mathbf{n}_i = [n_i^x, n_i^y, n_i^z]^T$
ϵ_i	Random error term, $N(0, \tau^2)$ distributed.
τ^2	Variance of ϵ_i

However, the geometric precision of 3D scanning, especially non-contact methods, is still debatable for the above applications [10]. RE is often utilized in medical applications [20] or aerospace applications [21], requiring the final products with high accuracy and precision. Since 3D scanning is the first step of RE, the precision of the collected point clouds is critical for the whole process. On the other hand, the quality inspection also requires high-precision scanning. Its variability will heavily influence the following decision-making regarding quality and process improvement.

Although accuracy is recognized as a critical consideration in 3D scanning or RE technologies, in this study we focus on reducing variance to get a high-precision point cloud. The geometric metrology hardware is assumed to be well-calibrated before scanning, if it is not NIST-traceable.

To improve the quality of the 3D scanned point cloud, factors that have an impact on the precision and accuracy of the scanning process need to be identified. Then, an implicit functional relationship between these factors and a metric of the quality characteristic, e.g., precision or variance, is required to assist in identifying the potential solution that could improve

the quality of the scanning process and, further, increase the precision of the point clouds. Next, an optimization procedure can help to optimize the scanning strategy with respect to the solution or factors identified.

In this paper, Section 2 first reviews the geometric factors that could influence the geometric precision of the scanning process and the variance model of the point cloud using these factors. Within this model, a controllable factor, the points' normal directions, is identified in Section 3, which could potentially reduce the point cloud variability. A Bayesian optimization model is adopted to minimize the variances with respect to the normal direction. Section 4 presents case studies with three geometrically different parts printed by AM to validate the proposed framework.

2. Point Cloud Variance Modeling

Many non-contact scanning methods are available for industrial applications [10]. This study focuses on utilizing a laser scanner for RE or quality inspection purposes since it has a high precision for manufacturing-related applications.

The mechanism of a laser scanner is to project laser strips onto the surfaces of the target object [22]. A charge-coupled device (CCD) camera captures the reflected laser strips and records the point spatial information by the laser-projected location on the receiver. Therefore, the 3D-scanned point cloud variances are heavily influenced by the interferences that happen on the object's surfaces, presented in Figure 1. Since the interferences of a survey point are caused by its near neighborhood, two critical local geometric factors are identified by Geng et al. [23], which are the point's normal directions and local curvature change. The authors propose a Bayesian extreme learning machine (BELM) to model the functional relationship between point variances and these two local geometric descriptors. In this paper, we briefly review their model, which later can be utilized to find the best scanning posture.

Many factors could influence the variance of the surveyed point cloud, which are presented in Figure 2; however, factors, such as scanner hardware or environment, are “controllable” factors that can be changed and set at the optimal level.

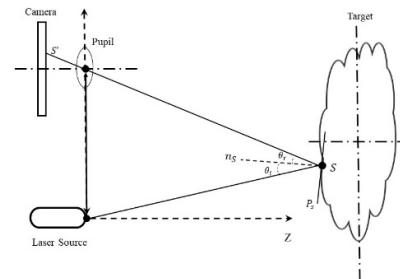


Figure 1. Mechanism of a laser scanner with a single laser stripe. Here P_S is the tangent plane of the surface at the point S and n_S indicates the normal direction. The incident angle θ_i equals the reflection angle θ_r [23].

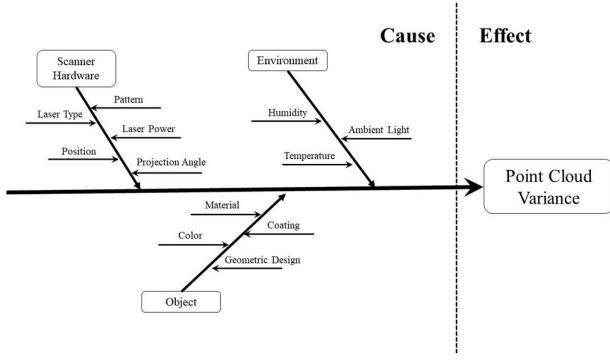


Figure 2. Fishbone diagram of a sample of factors related to the measured objects, scanning hardware, and environments that could influence the variance of a laser scanner [23].

Many other factors, such as ambient light, the object's color, and the material's reflectance rate, could also affect the scanning variance. However, these factors can be seen as controllable factors for the scanning process that can be set at optimal conditions [24]. On the other hand, the geometric shape of the target object cannot be standardized. These uncontrollable factors, especially the geometric design of the scan target, are either fixed or cannot be directly changed in a scanning project. Thus, it is critical to find the relationship between the geometric design and the variance of the point cloud. Therefore, our variance model focuses on building the relationship between these geometric descriptors and the point variances.

The mechanism of a general laser scanner is presented in Figure 1. The Law of Reflection states that the incident angle θ_i should always equal the angle of reflection θ_r . Therefore, if the point's normal direction is orthogonal to the incident laser strip, this point can be difficult to be captured on the CCD camera, which may increase the variance of this point. Furthermore, it is not easy to accurately measure the point in the high-curvature area. The reason is that the points in or near high curvature areas are generally located in a small region. These points are also difficult to capture by the laser strips because their tangent planes and normals are relatively more sensitive to noise due to high curvature.

One unique observation from the 3D scanning process is the variances of the z -coordinate are much higher than those of the rest two coordinates. Therefore, we only focus on the model and posture optimization with respect to the z -coordinates in this study. The z -coordinate variances can be modeled as

$$t_i = f(\cos(\theta_i), v_i) + \varepsilon_i, \quad (1)$$

where $i = 1, \dots, n$ is the index for the points, $t_i = \log(\sigma_i^2)$ is the outcome variable that corresponds to the logarithmic transformation of the variance for the z -coordinate of the point i , θ_i is the angle between the normal direction vector of the point i and the vertical axis, v_i is the rate of the local curvature

change of point i , and the error terms ε_i are independent $N(0, \tau^2)$ random variables and τ^2 is the variance of ε_i .

Since this functional relationship can be highly nonlinear, and the functional form between the predictors and response is unknown, a flexible model that could approximate this implicit relationship should be selected. The BELM model is adopted for functional approximation as it can be seen as a universal approximation to any functional forms [25]. This model is a single-layer feedforward neural network whose input weights are randomly assigned by a predetermined distribution. Since the volume of the point clouds is large (millions or even billions), the general flexible, nonparametric regression methods, such as Gaussian processes, random forests, neural networks, etc., can cost a huge amount of computational resources and a long time to fit the data to the model. BELM, on the other hand, can reduce the complex model training procedure in the neural network, such as gradient descent, to fitting a linear regression model, which is computationally efficient while flexible enough to approximate the implicit functional form.

3. Posture Optimization for Variance Minimization

This section proposes a framework based on the BELM variance model to seek the object's best posture to minimize the variance measure. In the variance model presented in Section 2, two local geometric descriptors are selected as inputs: the point's local curvature change and normal direction. The first one is a constant with respect to the object. Since the mechanical parts are treated as rigid objects, their physical form is fixed. Thus, the local curvature change measures are invariable to the measured points. Even though the scanner could avoid these high curvature areas to reduce the variance, these areas usually play critical functional roles, which calls for much denser measurement.

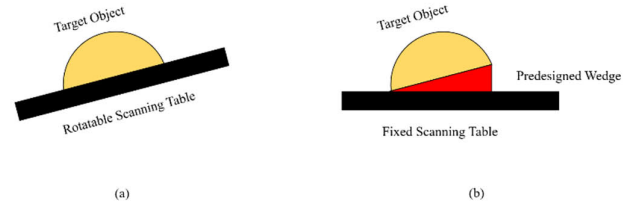


Figure 3. Proposed strategies to reduce the scanning variability: (a) the target object is placed on a rotatable scanning table, which provides the scanner with the target at the optimal scanning posture, and (b) the target object is attached to a predesigned wedge, whose shape is designed via the proposed Bayesian optimization model, on a fixed scanning table.

The normal direction is controllable by rotating the scanning table (Figure 3 (a)) or by providing a specialized fixture design (Figure 3 (b)). Let the standardized normal direction of the point i be $n_i = [n_i^x, n_i^y, n_i^z]^T$, $i = 1, \dots, n$, and the general rigid rotation matrix R can be written as

$$R = \begin{bmatrix} \cos\alpha\cos\beta & \cos\alpha\sin\beta\sin\gamma - \sin\alpha\cos\gamma & \cos\alpha\sin\beta\cos\gamma + \sin\alpha\sin\gamma \\ \sin\alpha\cos\beta & \sin\alpha\sin\beta\sin\gamma + \cos\alpha\cos\gamma & \sin\alpha\sin\beta\cos\gamma - \cos\alpha\sin\gamma \\ -\sin\beta & \cos\beta\sin\gamma & \cos\beta\cos\gamma \end{bmatrix}, \quad (2)$$

where α, β, γ are yaw (z -axis), pitch (y -axis), and roll (x -axis) rotation angles. Therefore, the new normal direction of any point i on the object is Rn_i . Notice that, in the BELM model, θ_i is the angle between n_i and the vertical axis, so $\cos(\theta_i) = n_i \cdot z$, where $z = [0, 0, 1]^T$. After rotation, the cosine value of the new angle becomes $\cos(\theta_i^R) = (Rn_i) \cdot z$, which can be written as

$$\cos(\theta_i^R) = -\sin\beta \ n_i^x + \cos\beta \ \sin\gamma \ n_i^y + \cos\beta \ \cos\gamma \ n_i^z \quad (3)$$

One insight from this formula is that the yaw rotation angle α —or rotation angle about z -axis—will not influence the points' variances. This is intuitive since the rotation about z -axis is the same as the translation on the scanning table, which is not considered as an influencing factor (Figure 2).

Therefore, our optimization model can be written as follows,

$$\min_{\beta, \gamma} \max_{i \in \{1, \dots, n\}} \hat{f}(\theta_i^R, v_i) \quad (4)$$

$$s.t. \quad -\pi \leq \beta \leq \pi$$

$$-\pi \leq \gamma \leq \pi$$

where $\hat{f}(\theta_i^R, v_i)$ is the BELM model trained by the proposed method in [23]. Since the objective function is the fitted BELM model, a “black-box” model, a Bayesian optimization technique is utilized to solve this minimization problem. Bayesian optimization is a class of optimization methods that utilize a surrogate model in place of the expensive black-box derivative-free objective function. A Gaussian process regression model is usually adopted as the surrogate, and an acquisition function is implemented to explore the parameter space and find the global optimum [26]. In this study, we reformulate the original constrained-minimax problem as a minimization model of an expensive function with a rectangle parameter space, which can be written as

$$\min_{\beta, \gamma \in [-\pi, \pi]} g(\beta, \gamma), \quad (5)$$

where $g(\beta, \gamma) = \max_{i \in \{1, \dots, n\}} \hat{f}(\theta_i^R, v_i)$. This problem can be solved by a Bayesian optimization algorithm with the expected improvement as the acquisition function. One trivial but critical point is that, while the Bayesian optimization algorithm could solve this “black-box” model, the maximization function over $i \in \{1, \dots, n\}$ is not a continuous, smooth function, which, technically, cannot be approximated by the Gaussian processes model. Therefore, we utilize the softmax function in place of the strict maximization to make the objective function smooth,

$$g'(\beta, \gamma) = \sum_{i=1}^n \frac{\exp(\hat{f}(\theta_i^R, v_i))}{\sum_{j=1}^n \exp(\hat{f}(\theta_j^R, v_j))} \exp(\hat{f}(\theta_i^R, v_i)) \quad (6)$$

It is well known that the softmax function is continuous everywhere [27] that can be approximated by Gaussian processes. The basic procedures of the Bayesian optimization are presented in Algorithm 1, which can be solved using the Bayesian Optimization package in Python [28]. Intuitively, Bayesian optimization is a sequential optimization algorithm, where an acquisition function helps to explore the feature space and find the region with the highest uncertainty. In this study,

we utilize the expected improvement function as the acquisition function, and the algorithm will stop after N steps.

Algorithm 1: Basic procedures for Bayesian optimization

Adopt a Gaussian process model as prior for

$$g(\beta, \gamma) = \max_{i \in \{1, \dots, n\}} \hat{f}(\theta_i^R, v_i).$$

Initialize the algorithm by random observing n_0 points in the parameter space and observe their function value.

Set $n = 0$.

while $n = 1$ **to** N **do**

Train the Gaussian process model using all the available data.

Let β_n, γ_n be a minimizer of the current expected improvement function.

Observe $g(\beta_n, \gamma_n)$.

$n \rightarrow n + 1$.

end

Return the β^*, γ^* with the smallest $g(\beta^*, \gamma^*)$ value.

4. Case Study

We now apply our variance minimization model to seek the optimal posture of the AM-printed freeform designs. Our study consists of three objects shown in Figure 3: one Half-Ball and two freeform objects. These three parts are printed using the LulzBot TAZ FDM machine, based on the filament deposition modeling process, with a gold metallic 2.85 mm polymer. Each part is scanned 30 times independently using a FARO Platinum 8' Arm Laser Scanner to train the BELM model. For each scanning trial, the optimal posture is also calculated utilizing the proposed Bayesian optimization procedure and a scan follows for the optimized scanning posture. We adopt the residual-BELM structure proposed in [23] as the model to fit the training data. Each of the residual-BELM had 20 layers for each of the 5 stack-up BELM models.

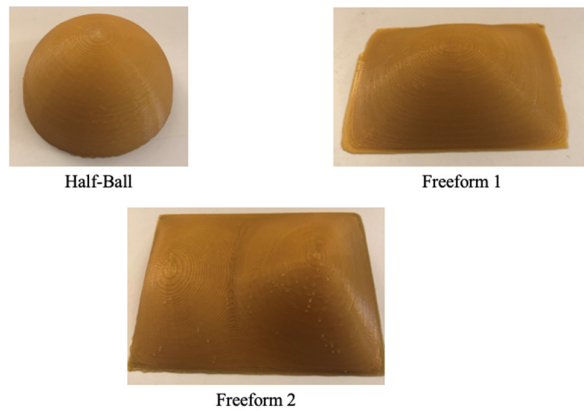


Figure 3. AM-printed parts that are considered in our case study

Our proposed Bayesian optimization model with softmax approximation and expected improvement function is applied to each scan to compare the performances between the original flat position and the optimal posture. The results are presented in Figure 4, which are the deviations between the scanned point clouds and the point clouds collected from Renishaw's coordinate measuring machine, which is both high accuracy and high precision. From these results, the optimized posture has much smaller deviations than the flat position for any scan of each object. However, the deviation reductions are not uniform for the subjects. This is because the distributions of the normal direction are different among the three objects. The Half-Ball has normal directions orthogonal to the vertical direction at its bottom area, while the bottom areas of the rest two are flatter than that of the Half-Ball. According to the scanning mechanism presented in Figure 2, if the normal direction is orthogonal to the laser projection direction, then the points around this area can be hard to survey since it is difficult to collect the reflection laser stripe. Therefore, rotating the Half-Ball object could significantly reduce the area that has a point normal orthogonal to the laser projection direction; while the other two objects, whose shapes are mostly flat, may not have significant improvement as the Half-Ball.

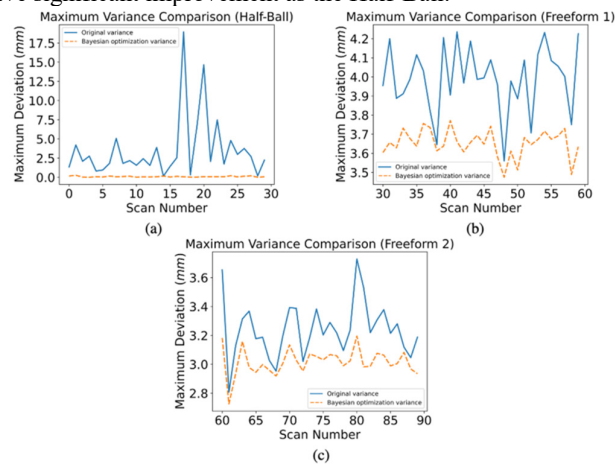


Figure 4. Maximum variances of the original position and optimized posture of each experimental object: (a) Half-Ball; (b) Freeform 1; and (c) Freeform 2

5. Conclusion

This paper presents a framework to reduce and minimize the variability of the 3D scanning process. We build a functional relationship between the measured-point variances and the local geometric descriptor based on the basic mechanism of a laser scanner. Under this relationship, we find one controllable factor, the point's normal direction, that could potentially reduce the scanning variability. We propose an optimization model to minimize the points' variances based on the variance model in the form of a BELM using Bayesian optimization. The proposed variance modeling technique is versatile in that it learns the scanner's behavior and utilizes this knowledge to increase the scanning performance.

One potential issue that was not addressed in our current study is the effect of rotation on the variance changes of the x - and y -coordinates. Even though the z -coordinate has more variability than the other two, the coordinate system may change after rotating the object. In our future work, all the coordinates will be considered simultaneously in the optimization model. A multi-objective Bayesian optimization technique will be investigated for such a problem to further reduce the scanning variance.

Acknowledgements

The work of Zhaohui Geng was supported by the National Institute of Standards and Technology under Grant No. 70NANB21H038.

References

- [1] Boehler, W. and A. Marbs, *3d Scanning Instruments*. Proceedings of the CIPA WG, 2002. **6**(9).
- [2] Bidanda, B., V. Narayanan, and R. Billo, *Reverse Engineering and Rapid Prototyping*. Handbook of Design, Manufacturing and Automation, 1994: p. 977-990.
- [3] Vermeulen, M.M.P.A., P. Rosielle, and P. Schellekens, *Design of a High-Precision 3d-Coordinate Measuring Machine*. Cirp Annals, 1998. **47**(1): p. 447-450.
- [4] Weckenmann, A., M. Knauer, and H. Kunzmann, *The Influence of Measurement Strategy on the Uncertainty of Cmm-Measurements*. CIRP Annals, 1998. **47**(1): p. 451-454.
- [5] Sladek, J., et al., *The Hybrid Contact-Optical Coordinate Measuring System*. Measurement, 2011. **44**(3): p. 503-510.
- [6] Feng, H.-Y., Y. Liu, and F. Xi, *Analysis of Digitizing Errors of a Laser Scanning System*. Precision Engineering, 2001. **25**(3): p. 185-191.
- [7] Billo, R.E., B. Bidanda, and D. Tate, *A Genetic Cluster Algorithm for the Machine-Component Grouping Problem*. Journal of Intelligent Manufacturing, 1996. **7**(3): p. 229-241.
- [8] Rajgopal, J. and B. Bidanda, *On Scheduling Parallel Machines with Two Setup Classes*. International Journal of Production Research, 1991. **29**(12): p. 2443-2458.
- [9] Hu, G., et al., *An Oligopoly Model to Analyze the Market and Social Welfare for Green Manufacturing Industry*. Journal of cleaner production, 2014. **85**: p. 94-103.
- [10] Geng, Z. and B. Bidanda, *Review of Reverse Engineering*

Systems—Current State of the Art. Virtual and Physical Prototyping, 2017. **12**(2): p. 161-172.

[11] Zang, Y. and P. Qiu, *Phase I Monitoring of Spatial Surface Data from 3d Printing*. *Technometrics*, 2018. **60**(2): p. 169-180.

[12] Li, L., et al., *An Integrated Approach of Reverse Engineering Aided Remanufacturing Process for Worn Components*. *Robotics and Computer-Integrated Manufacturing*, 2017. **48**: p. 39-50.

[13] Anwer, N. and L. Mathieu, *From Reverse Engineering to Shape Engineering in Mechanical Design*. *CIRP Annals*, 2016. **65**(1): p. 165-168.

[14] Pérez-Castillo, R., et al., *Reengineering Technologies*. *IEEE software*, 2011. **28**(6): p. 13-17.

[15] Wu, S., et al. *Agent-Based Discrete Event Simulation Modeling for Disaster Responses*. in *IIE Annual Conference. Proceedings*. 2008. Institute of Industrial and Systems Engineers (IISE).

[16] Balaban, C., et al., *Dynamic Discrete Decision Simulation System*. 2012, Google Patents.

[17] Geng, Z. and B. Bidanda, *Geometric Precision Analysis for Additive Manufacturing Processes: A Comparative Study*. *Precision Engineering*, 2021. **69**: p. 68-76.

[18] Gibson, I., et al., *Additive Manufacturing Technologies*. Vol. 17. 2021: Springer.

[19] Colosimo, B.M., et al., *Opportunities and Challenges of Quality Engineering for Additive Manufacturing*. *Journal of Quality Technology*, 2018. **50**(3): p. 233-252.

[20] Geng, Z. and B. Bidanda, *Medical Applications of Additive Manufacturing*, in *Bio-Materials and Prototyping Applications in Medicine*. 2021, Springer. p. 97-110.

[21] Gao, J., et al., *An Integrated Adaptive Repair Solution for Complex Aerospace Components through Geometry Reconstruction*. *The International Journal of Advanced Manufacturing Technology*, 2008. **36**(11): p. 1170-1179.

[22] Geng, Z., A. Sabbaghi, and B. Bidanda, *Reconstructing Original Design: Process Planning for Reverse Engineering*. *IISE Transactions*, 2022(just-accepted): p. 1-29.

[23] Geng, Z., A. Sabbaghi, and B. Bidanda, *Automated Variance Modeling for Three-Dimensional Point Cloud Data Via Bayesian Neural Network*. *IISE Transactions (Under Revision)*, 2021.

[24] Creehan, K.D. and B. Bidanda, *Computer-Aided Reverse Engineering of the Human Musculoskeletal System*. *Virtual and Physical Prototyping*, 2006. **1**(2): p. 83-91.

[25] Huang, G.-B., Q.-Y. Zhu, and C.-K. Siew, *Extreme Learning Machine: Theory and Applications*. *Neurocomputing*, 2006. **70**(1-3): p. 489-501.

[26] Frazier, P.I., *A Tutorial on Bayesian Optimization*. arXiv preprint arXiv:1807.02811, 2018.

[27] Goodfellow, I., Y. Bengio, and A. Courville, *Deep Learning*. 2016: MIT press.

[28] Nogueira, F., *Bayesian Optimization: Open Source Constrained Global Optimization Tool for Python; 2014*. URL <https://github.com/fmfn/BayesianOptimization>, 2020.